Designing CIGS solar cells with front-side point contacts

G. Sozzi[1], D. Pignoloni[1], R. Menozzi[1], F. Pianezzi[2], P. Reinhard[2], B. Bissig[2], S. Buecheler[2], A. N. Tiwari[2]

[1] Department of Information Engineering - University of Parma
Parco Area delle Scienze 181A, 43124 Parma, Italy

[2] Laboratory for Thin Films and Photovoltaics, Empa - Swiss Federal Laboratories for Materials Science and Technology, Ueberlandstrasse 129, CH-8600 Duebendorf, Switzerland.

Abstract - **In this work we show how 2D numerical simulations can be used to design and optimize front-side point contacts in surface-passivated CIGS cells. Detailed analysis of the combinations of passivation thickness, point contact size and pitch can help identifying solutions able to boost the performance of otherwise surface-limited cells: efficiencies close to those of cells with ideal (i.e., trap-free) CdS/CIGS interface can be achieved by the optimization of point contact features in the low nm range. The effect of varying the CIGS and CdS doping densities on the cell performance has also been analyzed.**

Index Terms — **CIGS passivation layer, point contact, thin-film photovoltaics.**

I. Introduction

Copper indium gallium diselenide $Cu(In_{1-x}Ga_x)Se_2$ (CIGS) is one of the most promising semiconductor materials for low cost, high efficiency thin-film solar cells. However, in order to reach the high efficiency/cost ratio the market requests, continuous improvement is a necessary task [1]. To achieve this goal, one first needs to identify the main electronic and optical loss mechanisms limiting the state-of-the-art solar cell performance, and, in a second step, to develop the best strategies to overcome these limits.

Non-radiative bulk and interface recombination is responsible for the main electrical losses in the cell [2], and is therefore among the first performance limiters to suppress. In order to reduce recombination at the interfaces between the CIGS absorber layer and the buffer and/or the bottom contact, passivation layers can be deposited, as for Si solar cells. CIGS cells with passivation at the rear surface combined with micron–sized openings (point contacts), showed increased efficiency for CIGS absorbers with reduced thickness [3].

However, the front CIGS surface (buffer/absorber interface) may also benefit from passivation, especially when the band alignment is less favorable than that of CdS [4]. Good passivation ensures minimal surface recombination losses in two ways: (i) it reduces interface defects, impurities or dangling bonds at the CIGS surface (chemical passivation); (ii) the presence of high negative fixed charge density inside the passivation repels minority carriers from the semiconductor interface (field-effect passivation) [5]. However, a passivation layer covering the whole absorber surface will result in large series resistance, which will cause the fill factor (FF) to drop. The insertion of point contacts at the front CIGS surface can – at least in part - overcome the problem, but it is necessary to determine the ideal point contact size and pitch, and the optimum passivation film thickness. A first experimental example of such type of point openings through a surface layer on top CIGS was recently discussed in ref. [6].

The present work investigates the effect of passivation with point contacts at the CIGS front surface by means of 2D numerical simulations where we vary (i) the passivation layer thickness, (ii) the point contact width and (iii) pitch. The effect of CdS and CIGS doping on cell performance has also been analyzed. The final aim is to provide guidelines for designing high-efficiency solar cells, with optimized geometrical features as determined by the 2D device simulations.

II. Methods

A. Simulations

We simulated the cell using the Synopsys Sentaurus-Tcad suite [7]. The cell behavior in the dark is described by the Poisson, electron and hole continuity, and drift-diffusion equations. Recombination via deep defects follows the Shockley – Read – Hall (SRH) model. The cell is illuminated by the standard AM1.5G solar spectrum.

Unlike in previous studies [8], here we consider a monocrystalline cell structure, because our analysis was focused on analyzing the effect of passivation and point contacts at the CdS buffer/CIGS interface. In addition to that, we will show that optimum point contact sizes are in the low nanometer range, which is much smaller than the average grain size.

The simulated cell is shown in Fig. 1. The passivation layer thickness h, the point contact width wpc, and pitch d are varied in order to evaluate their effect on cell performance. When $h = 0$, the CdS covers the full CIGS surface, and the cell structure is the standard one (i.e., with neither passivation nor point contacts). The most significant material parameters [9], [10] for the various cell layers are given in Table I, while the choice of passivation layer parameters is addressed below.

B. Simulation Scenarios

All simulations include spatially uniform bulk recombination centers; as far as interface recombination is concerned, we examined two scenarios for the CdS/CIGS

interface: ideal interface (no trap centers) and non-ideal interface (with trap centers).
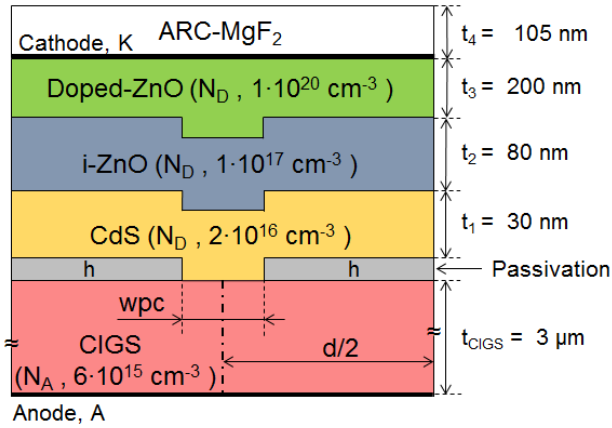

Fig. 1. Cross-section of the simulated solar cell (not to scale).

TABLE I
MATERIAL PARAMETERS USED IN THE SIMULATIONS

Material	ZnO	CdS	CIGS
Eg [eV]	3.3	2.4	1.21
$\varepsilon/\varepsilon_0$	9	9	10
Nc [cm^{-3}]	2.27×10^{18}	0.677×10^{18}	2.30×10^{18}
Nv [cm^{-3}]	3.34×10^{19}	1.53×10^{19}	1.80×10^{19}
μe [cm^2/(V·s)]	100	100	100
μh [cm^2/(V·s)]	25	25	25
τe [ns]	10	33	150
τh [ns]	25	25	25

We started setting the baseline for the standard cell with $h = 0$ − i.e., no passivation - in the case of ideal CdS/CIGS interface; the simulated cell efficiency is 20.7%. This value is close to the 20.4% measured on record cells [11] (which does not imply that surface recombination is absent in the record cell of ref. [11], since similar values of efficiency may result from different combinations of absorber and interface properties).

We then added an acceptor trap density of $3 \cdot 10^{11}$ cm^{-2} at the CdS/CIGS interface lowering the efficiency to η = 11.1%. The acceptors are located at the CIGS mid-gap, and give electron and hole lifetimes of 3.33 ps; these correspond to surface recombination velocity in the range of 10^6 cm/s. The simulated figures of merit of the baseline ($h = 0$) cell with and without acceptor traps at the CdS/CIGS interface under AM1.5G illumination are given in Table II, together with measured data from [11].

The performance of the baseline cell with ideal interface is therefore bulk-limited, while that of the cell with CdS/CIGS interface acceptors is interface-limited.

In order to recover from the 11.1% efficiency of the interface-limited scenario, we simulated structures with passivation of thickness $h = 5$ nm, 10 nm, 25 nm on the upper CIGS surface (see Fig. 1); we assume that this layer completely passivates the surface acceptor traps, which are therefore only present in the point contact surface. The bandgap of the passivation (Eg = 5 eV) is chosen so that it is transparent to the incident light, with a spike on the conduction band ($\Delta E_C = 0.5$ eV) at the interface with CIGS.

For each value of the passivation thickness h, we considered three values of the point contact pitch d, namely, 50 nm, 100 nm, and 250 nm. Finally, for each combination of h and d, we vary the point contact width wpc between 5 nm and ($d - 10$ nm).

TABLE II
BASELINE ($h = 0$) CELL PARAMETERS UNDER AM1.5G ILLUMINATION.

	V_{oc} [V]	J_{sc} [mA/cm^2]	FF [%]	η [%]
Simulated (ideal interface)	0.734	35.1	80.3	20.7
Simulated (non-ideal interface)	0.579	34.7	55.4	11.1
Measurement [11]	0.736	35.1	78.9	20.4

III. RESULTS AND DISCUSSION

The best efficiency for each value of passivation thickness h and the corresponding combination of d and wpc values is shown in Table III.

TABLE III
CELL PARAMETERS UNDER AM1.5G ILLUMINATION

Non – ideal interface			
h [nm]	optimum d [nm]	optimum wpc [nm]	η [%]
5	50	5	19.59
10	50	5	18.99
25	50	5	17.17

We observe the best performance in Tab. III for the thinnest ($h = 5$ nm) passivation, in conjunction with narrow ($wpc = 5$ nm) and closely spaced ($d = 50$ nm) point contacts.

Looking at Fig. 2, we observe that, in the presence of interface acceptor traps, narrow point contacts – i.e., with small wpc - yield Jsc and Voc values very close to the ideal ones, but give a smaller benefit to FF, which remains significantly lower than that of the baseline cell without interface traps.
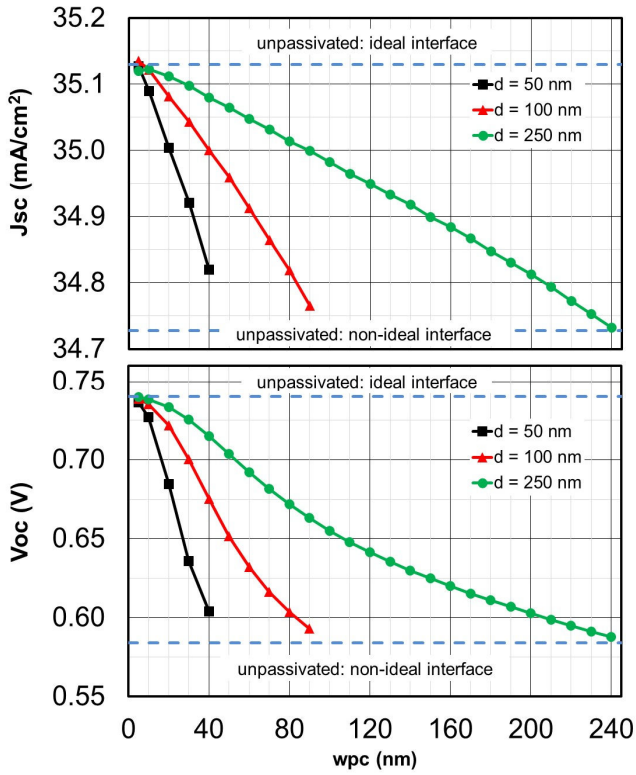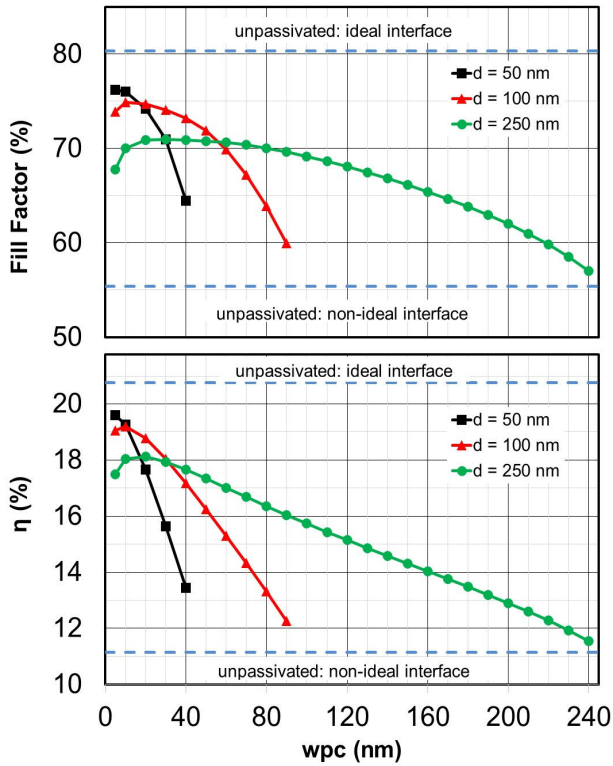
Fig. 2: Simulated cell parameters vs. point contact width, *wpc*, for varying pitch, *d*. Non-ideal interface. *h* = 5 nm. The two reference lines indicate the case of absence of interface states (top line) and the case of presence of interface states with no passivation (bottom line).

The cell performance appears thus to be limited by the series resistance arising from the current path inside the absorber - larger point contact pitch *d* implies higher resistance - which adds to the parasitic resistance of narrow point contacts. This parasitic resistance increases with passivation thickness, too, because the CdS thickness covering the point contact corners – which is equal to (30 nm – *h*), as seen in Fig. 1 - is reduced for higher *h*, thus determining the simulated dependence of cell performance on *h* (see Tab. III).
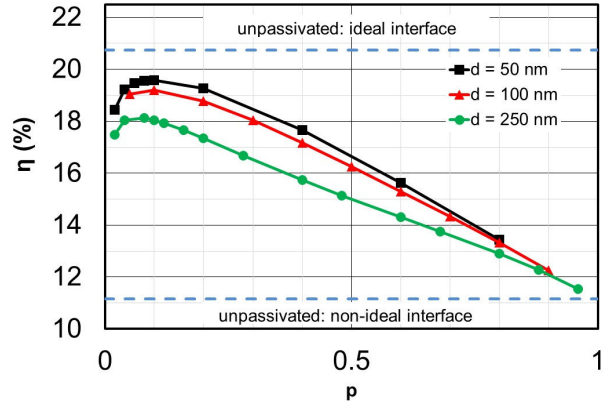

Fig. 3: Simulated efficiency η versus *p* (*p* = *wpc/d*), for varying point contact pitch, *d*. *h* = 5 nm.

If *p* is the ratio between the point contact width *wpc* and the distance *d* between point contacts, *p* = *wpc/d,* we can see from Fig. 3 that there is an optimum value of *p* that maximizes the efficiency η, namely, *p* = 0.1.

It is important to point out that, unlike the case of Si cells, where micron-size or larger point contacts are used [12], our CIGS case calls for features in the lower nm range. This requires challenging patterning strategies, but the feasibility of such nano-patterned point contacts at the front CIGS interface has been recently demonstrated [6].

We have shown so far that the optimum point contact pattern is the result of a trade-off between the beneficial effect of surface acceptor passivation, which is maximum for narrow point contacts and wide pitch, and the detrimental effect of series resistance, which gets worse as the point contacts are made narrower and wider apart. It is therefore interesting to evaluate the effect of increased doping densities on the structures with point contacts, since it may be expected that more conductive CIGS and/or CdS layers would make the cell suffer less from series resistance effects, thus enhancing the point contact benefits.

With reference to a cell with *h* = 5 nm, *d* = 50 nm, *wpc* = 5 nm, we have simulated the illuminated behavior for different values of the CIGS acceptor doping density, while keeping the CdS donor doping density fixed at 2×10^{16} cm^{-3}. The effects on cell performance are negative, as shown in Fig. 4.
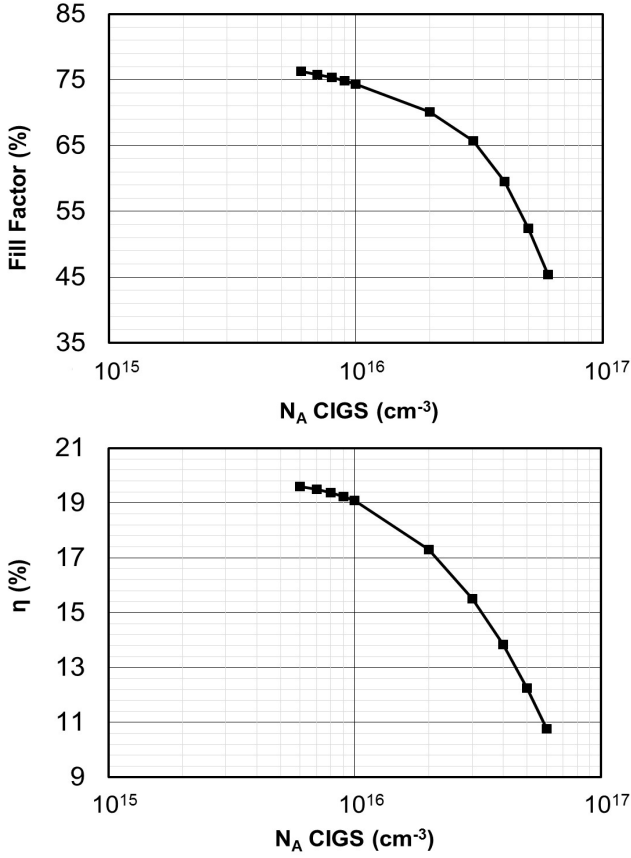
Fig. 4: Simulated cell parameters vs. CIGS acceptor doping density. Non-ideal interface. h = 5 nm, d = 50 nm, wpc = 5 nm. The CdS donor doping density is 2×10^{16} cm^{-3}.
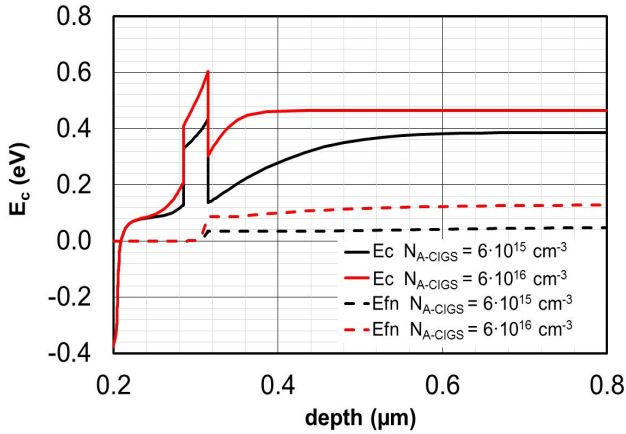

Fig. 5: Conduction band profile and electron quasi-Fermi levels at 0.601 V and AM1.5 (maximum power point for the cell with 6×10^{15} cm^{-3} CIGS doping) for two different values of CIGS acceptor doping density (legend). Non-ideal interface. h = 5 nm, d = 50 nm, wpc = 5 nm. The CdS donor doping density is 2×10^{16} cm^{-3}.

An explanation for the FF drop can be found in the band profiles of Fig. 5: heavier CIGS acceptor doping results in larger voltage drop across the CdS buffer, i.e., an increase of series resistance that drastically affects FF (see [4] for a discussion of the effects of doping and band alignment on CIGS cells performance): the voltage drop in the CdS layer under these conditions (0.601 V, AM1.5 illumination) almost doubles from 103 mV to 187 mV when the CIGS doping increases from 6×10^{15} to 6×10^{16} cm^{-3}.

Under short-circuit conditions, the CdS voltage drop is 159 mV for 6×10^{15} cm^{-3}, 339 mV for 6×10^{16} cm^{-3}.
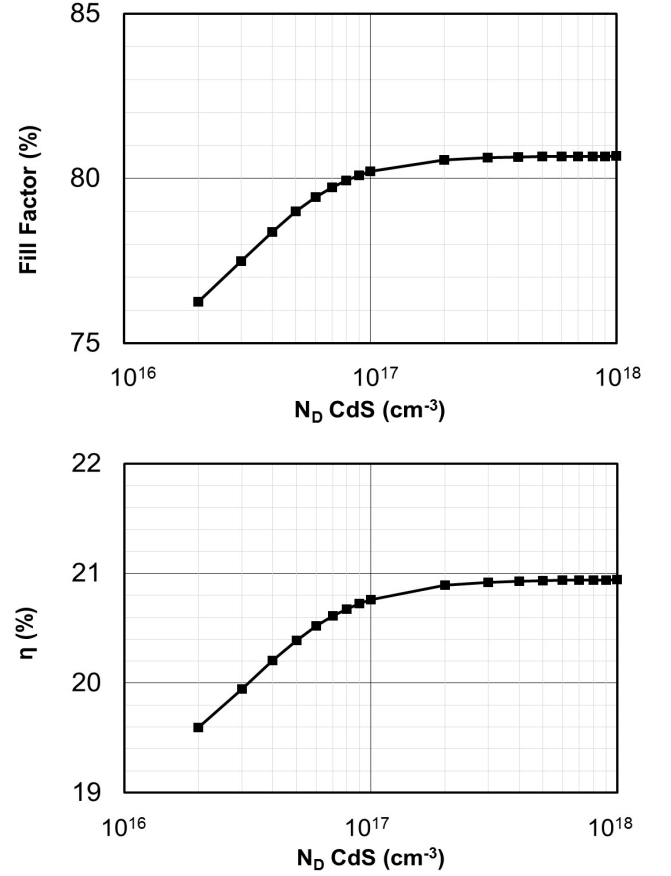

Fig. 6: Simulated cell parameters vs. CdS donor doping density. Non-ideal interface. h = 5 nm, d = 50 nm, wpc = 5 nm. The CIGS acceptor doping density is 6×10^{15} cm^{-3}.

On the other hand, increasing the CdS doping does prove successful, as shown by Fig. 6. Again, the effect on V_{OC} (+0.7%) and J_{SC} (+0.5%) is marginal, the benefit coming from FF due to the reduction of the parasitic series resistance.

VI. CONCLUSION

This work is focused on the use of 2D numerical simulations for the design and optimization of front-side point contacts in CIGS cells.

We show that careful analysis of the combinations of passivation thickness and point contact size and pitch can help salvaging the performance of otherwise surface-limited cells: efficiencies close to those of cells with ideal (i.e., trap-free) CdS/CIGS interface can be achieved by the optimization of point contact arrangement.

Our simulations show that features in the low nm range are required for optimal performance. Such nano-patterning of the cell's surface has been proven feasible by recently published work.

Finally, since the optimum point contact pattern geometry comes from a trade-off between the beneficial effect of surface acceptor passivation, which is maximum for narrow and widely separated point contacts, and the detrimental effect of series resistance, which increases as the point contacts are made narrower and wider apart, we have analyzed the effects of varying the CIGS and CdS doping densities. While increasing the acceptor doping of the absorber has a negative impact on the cell's fill factor and efficiency, due to degraded electron collection at the cathode, a heavier doping of the CdS buffer,and the attendant reduction of the point contact series resistance, bring significant benefit to the cell's performance.

References

[1] C. A. Wolden, J. Curtin, J. B. Baxter, I. Repins, S. E. Shaheen, J. T. Torvik, A. A. Rockett, V. M. Fthenakis, E. S. Aydil, "Photovoltaic manufacturing: present status, future prospects, and research needs", *Journal of Vacuum Science & Technology A*, vol. 29, 030801, 2011.

[2] U. Rau , A. Jasenek, H. W. Schock, F. Engelhardt, T. Meyer, "Electronic loss mechanisms in chalcopyrite based heterojunction solar cells", *Thin Solid Films*, vol. 361-362, pp. 298-302, 2000.

[3] B. Vermang, J. Timo Wätjen, V. Fjällström, F. Rostvall, M. Edoff, R. Kotipalli, F.Henry and D. Flandre, "Employing Si solar cell technology to increase efficiency of ultra-thin Cu(In,Ga)Se2 solar cells", *Progress in Photovoltaics: Research and Applications*, vol. 22, pp. 1023–1029, 2014.

[4] G. Sozzi , F. Troni, R. Menozzi, "On the combined effects of window/buffer and buffer/absorber conduction-band offsets, buffer thickness and doping on thin-film solar cell performance", *Solar Energy Materials & Solar Cells*, vol. 121, pp. 126–136, 2014.

[5] W.-W. Hsu, J. Y. Chen, T.-H. Cheng, S. C. Lu, W.-S. Ho, Y.-Y. Chen, Y.-J. Chien, and C.W. Liu, "Surface passivation of $Cu(In,Ga)Se_2$ using atomic layer deposited Al_2O_3", *Applied Physics Letters*, vol. 100, pp. 023508-1–023508-3, 2012.

[6] P. Reinhard, B. Bissig, F. Pianezzi, H. Hagendorfer, G. Sozzi, R. Menozzi, C. Gretener, S. Nishiwaki, S. Buecheler, A. N. Tiwari, "Alkali-templated surface nanopatterning of chalcogenide thin films: a novel approach toward solar cells with enhanced efficiency," *Nano Letters*, DOI: 10.1021/acs.nanolett.5b00584, Apr. 6, 2015 (Web).

[7] http://www.synopsys.com/Tools/TCAD.

[8] G. Sozzi, R. Mosca, M. Calicchio, R. Menozzi, "Anomalous dark current ideality factor (n > 2) in thin-film solar cells: the role of grain-bundary defects," *Proc. 40th IEEE Photovoltaic Specialist Conf. (PVSC)*, pp. 1718-1721, 2014.

[9] A. Chirilă, S. Buecheler, F. Pianezzi, P. Bloesch, C. Gretener, A. R. Uhl, C. Fella, R. Kranz, J. Perrenoud, S. Seyrling, R. Verma, S. Nishiwaki, Y. E. Romanyuk, G. Bilger, A. N. Tiwari, Highly efficient $Cu(In,Ga)Se_2$ solar cells grown on flexible polymer films, *Nature Materials*, vol. 10, pp. 857-861, 2011.

[10] R. Scheer, Towards an electronic model for $CuIn_{1-x}Ga_xSe_2$ solar cells, *Thin Solid Films*, vol. 519, pp. 7472–7475, 2011.

[11] A. Chirilă, P. Reinhard, F. Pianezzi, P. Bloesch, A. R. Uhl, C. Fella, L. Kranz, D. Keller, C. Gretener, H. Hagendorfer, D. Jaeger, R. Erni, S. Nishiwaki, S. Buecheler and A. N. Tiwari, "Potassium-induced surface modification of $Cu(In,Ga)Se_2$ thin films for high-efficiency solar cells", *Nature Materials,* vol. 12, pp. 1107–1111, 2013.

[12] A. Cacciato, F. Duerinckx, K. Baert, M. Moors, T. Caremans, G. Leys, M. Mrcarica, E. Picard, A. Ristow, and J. Szlufcik, "Industrial PERL-type Si solar cells with efficiencies exceeding 19.5%," *Journal of Photovoltaics*, vol. 3, pp. 628-634, 2013.